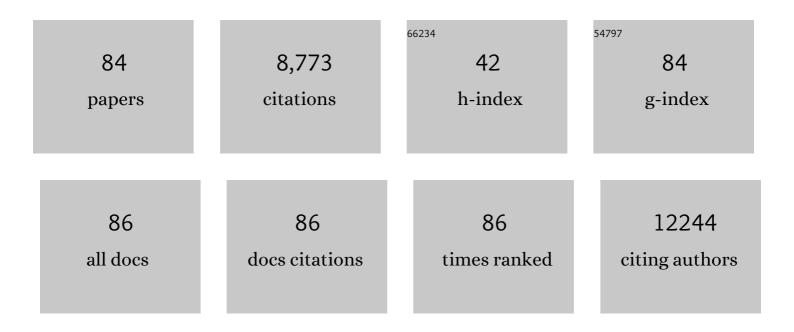


List of Publications by Year in descending order

Source: https://exaly.com/author-pdf/2312662/publications.pdf Version: 2024-02-01



Ιτικι Χτι

#	Article	IF	CITATIONS
1	Construction of amorphous Fe0.95S1.05 nanorods with high electrocatalytic activity for enhanced hydrogen evolution reaction. Electrochimica Acta, 2022, 402, 139554.	2.6	6
2	Facile synthesis of ZnO/PdSe2 core-shell heterojunction for efficient photodetector application. Chemical Engineering Journal, 2021, 413, 127484.	6.6	14
3	Sandwiched Cathodes Assembled from CoS ₂ â€Modified Carbon Clothes for Highâ€Performance Lithiumâ€Sulfur Batteries. Advanced Science, 2021, 8, e2101019.	5.6	64
4	Constructing CdS-Based Electron Transporting Layers With Efficient Electron Extraction for Perovskite Solar Cells. IEEE Journal of Photovoltaics, 2021, 11, 1014-1021.	1.5	6
5	Nearâ€Infrared Photoactive Semiconductor Quantum Dots for Solar Cells. Advanced Energy Materials, 2021, 11, 2101923.	10.2	20
6	Metastable marcasite NiSe ₂ nanodendrites on carbon fiber clothes to suppress polysulfide shuttling for high-performance lithium–sulfur batteries. Nanoscale, 2021, 13, 16487-16498.	2.8	13
7	Sub-picosecond passively mode-locked thulium-doped fiber laser by ReS ₂ nanoparticles. Japanese Journal of Applied Physics, 2021, 60, 011001.	0.8	6
8	Enhanced performance of all solid-state quantum dot-sensitized solar cells <i>via</i> synchronous deposition of PbS and CdS quantum dots. New Journal of Chemistry, 2020, 44, 505-512.	1.4	3
9	Phase transformation and sulfur vacancy modulation of 2D layered tin sulfide nanoplates as highly durable anodes for pseudocapacitive lithium storage. Chemical Engineering Journal, 2020, 392, 123722.	6.6	46
10	Enhanced Sodium Storage Performance of Co ₇ Se ₈ Enabled Through Inâ€Situ Formation of a Nanoporous Architecture. ChemElectroChem, 2020, 7, 4361-4368.	1.7	1
11	Nanoscale engineering and Mo-doping of 2D ultrathin ReS ₂ nanosheets for remarkable electrocatalytic hydrogen generation. Nanoscale, 2020, 12, 17045-17052.	2.8	22
12	Transformation of Two-Dimensional Iron Sulfide Nanosheets from FeS ₂ to FeS as High-Rate Anodes for Pseudocapacitive Sodium Storage. ACS Applied Energy Materials, 2020, 3, 12672-12681.	2.5	20
13	Oxygen-Doped VS ₄ Microspheres with Abundant Sulfur Vacancies as a Superior Electrocatalyst for the Hydrogen Evolution Reaction. ACS Sustainable Chemistry and Engineering, 2020, 8, 15055-15064.	3.2	25
14	Vanadium-doping in interlayer-expanded MoS ₂ nanosheets for the efficient electrocatalytic hydrogen evolution reaction. Inorganic Chemistry Frontiers, 2020, 7, 2497-2505.	3.0	23
15	Multifunctional MoSe2@rGO coating on the cathode versus the separator as an efficient polysulfide barrier for high-performance lithium-sulfur battery. Applied Surface Science, 2020, 527, 146785.	3.1	49
16	Combinational modulations of NiSe ₂ nanodendrites by phase engineering and iron-doping towards an efficient oxygen evolution reaction. Journal of Materials Chemistry A, 2020, 8, 8113-8120.	5.2	82
17	Cu2SnS3 nanocrystals decorated rGO nanosheets towards efficient and stable hydrogen evolution reaction in both acid and alkaline solutions. Materials Today Energy, 2020, 17, 100435.	2.5	12
18	Electronics from solution-processed 2D semiconductors. Journal of Materials Chemistry C, 2019, 7, 12835-12861.	2.7	24

Jun Xu

#	Article	IF	CITATIONS
19	Commercial Upconversion Phosphors with High Light Harvesting: A Superior Candidate for Highâ€Performance Dye‧ensitized Solar Cells. Physica Status Solidi (A) Applications and Materials Science, 2019, 216, 1900382.	0.8	3
20	Synthesis of MOF-derived nanostructures and their applications as anodes in lithium and sodium ion batteries. Coordination Chemistry Reviews, 2019, 388, 172-201.	9.5	192
21	Oxygen-incorporated and layer-by-layer stacked WS ₂ nanosheets for broadband, self-driven and fast-response photodetection. Nanoscale, 2019, 11, 6810-6816.	2.8	21
22	Metallic 1T-VS ₂ nanosheets featuring V ²⁺ self-doping and mesopores towards an efficient hydrogen evolution reaction. Inorganic Chemistry Frontiers, 2019, 6, 3510-3517.	3.0	39
23	Three-dimensional MoS2/rGO foams as efficient sulfur hosts for high-performance lithium-sulfur batteries. Chemical Engineering Journal, 2019, 355, 671-678.	6.6	164
24	Carbon Quantum Dots–Modified Interfacial Interactions and Ion Conductivity for Enhanced High Current Density Performance in Lithium–Sulfur Batteries. Advanced Energy Materials, 2019, 9, 1802955.	10.2	102
25	A top-down synthesis of wurtzite Cu ₂ SnS ₃ nanocrystals for efficient photoelectrochemical performance. Journal of Materials Chemistry A, 2018, 6, 8221-8226.	5.2	19
26	Synergistic Interlayer and Defect Engineering in VS ₂ Nanosheets toward Efficient Electrocatalytic Hydrogen Evolution Reaction. Small, 2018, 14, 1703098.	5.2	180
27	Interlayer-expanded and defect-rich metal dichalcogenide (MX ₂) nanosheets for active and stable hydrogen evolution. Inorganic Chemistry Frontiers, 2018, 5, 3140-3147.	3.0	16
28	Copper selenide (Cu ₃ Se ₂ and Cu _{2â^'x} Se) thin films: electrochemical deposition and electrocatalytic application in quantum dot-sensitized solar cells. Dalton Transactions, 2018, 47, 16587-16595.	1.6	38
29	Green and room-temperature synthesis of aqueous CuInS2 and Cu2SnS3 nanocrystals for efficient photoelectrochemical water splitting. Materials Today Energy, 2018, 10, 200-207.	2.5	12
30	Interlayer Nanoarchitectonics of Twoâ€Dimensional Transitionâ€Metal Dichalcogenides Nanosheets for Energy Storage and Conversion Applications. Advanced Energy Materials, 2017, 7, 1700571.	10.2	303
31	Recent progress in layered metal dichalcogenide nanostructures as electrodes for high-performance sodium-ion batteries. Journal of Materials Chemistry A, 2017, 5, 7667-7690.	5.2	144
32	Conversion of 1T-MoSe ₂ to 2H-MoS _{2x} Se _{2â^2x} mesoporous nanospheres for superior sodium storage performance. Nanoscale, 2017, 9, 1484-1490.	2.8	104
33	Arrays of ZnSe/MoSe ₂ Nanotubes with Electronic Modulation as Efficient Electrocatalysts for Hydrogen Evolution Reaction. Advanced Materials Interfaces, 2017, 4, 1700948.	1.9	39
34	(SiC/AlN) ₂ multilayer film as an effective protective coating for sintered NdFeB by magnetron sputtering. Materials Research Express, 2017, 4, 086407.	0.8	3
35	Synthesis of double-shelled copper chalcogenide hollow nanocages as efficient counter electrodes for quantum dot-sensitized solar cells. Materials Today Energy, 2017, 5, 331-337.	2.5	23
36	Cu2ZnSnS4 and Cu2ZnSn(S1â^'xSex)4 nanocrystals: room-temperature synthesis and efficient photoelectrochemical water splitting. Journal of Materials Chemistry A, 2017, 5, 25230-25236.	5.2	24

Jun Xu

#	Article	IF	CITATIONS
37	Hierarchical nanotubes constructed from interlayer-expanded MoSe ₂ nanosheets as a highly durable electrode for sodium storage. Journal of Materials Chemistry A, 2017, 5, 24859-24866.	5.2	88
38	Arrays of ZnO/MoS2 nanocables and MoS2 nanotubes with phase engineering for bifunctional photoelectrochemical and electrochemical water splitting. Chemical Engineering Journal, 2017, 328, 474-483.	6.6	103
39	Sodium-ion nanomachining to shape microcrystals into nanostructures and tune their properties. RSC Advances, 2016, 6, 42223-42228.	1.7	1
40	Synthesis of 1T-MoSe ₂ ultrathin nanosheets with an expanded interlayer spacing of 1.17 nm for efficient hydrogen evolution reaction. Journal of Materials Chemistry A, 2016, 4, 14949-14953.	5.2	190
41	A top-down strategy to synthesize wurtzite Cu ₂ ZnSnS ₄ nanocrystals by green chemistry. Chemical Communications, 2016, 52, 9821-9824.	2.2	12
42	Composition and Interface Engineering of Alloyed MoS ₂ <i>_x</i> Se _{2(1–} <i>_x(i>₎ Nanotubes for Enhanced Hydrogen Evolution Reaction Activity. Small, 2016, 12, 4379-4385.</i>	5.2	72
43	A novel anion-exchange strategy for constructing high performance PbS quantum dot-sensitized solar cells. Nano Energy, 2016, 30, 559-569.	8.2	40
44	Hierarchical nanotubes assembled from MoS 2 -carbon monolayer sandwiched superstructure nanosheets for high-performance sodium ion batteries. Nano Energy, 2016, 22, 27-37.	8.2	333
45	Simple template fabrication of porous MnCo ₂ O ₄ hollow nanocages as high-performance cathode catalysts for rechargeable Li-O ₂ batteries. Nanotechnology, 2016, 27, 135703.	1.3	17
46	In Situ Carbon-Doped Mo(Se _{0.85} S _{0.15}) ₂ Hierarchical Nanotubes as Stable Anodes for High-Performance Sodium-Ion Batteries. Small, 2015, 11, 5667-5674.	5.2	101
47	Controllable Synthesis of Bandgapâ€Tunable CuS _{<i>x</i>} Se _{1â^'<i>x</i>} Nanoplate Alloys. Chemistry - an Asian Journal, 2015, 10, 1490-1495.	1.7	18
48	Pyrite FeS ₂ microspheres wrapped by reduced graphene oxide as high-performance lithium-ion battery anodes. Journal of Materials Chemistry A, 2015, 3, 7945-7949.	5.2	134
49	Arrays of ZnO/CuInxGa1â^'xSe2 nanocables with tunable shell composition for efficient photovoltaics. Journal of Applied Physics, 2015, 117, .	1.1	11
50	Water Evaporation Induced Conversion of CuSe Nanoflakes to Cu _{2â^'<i>x</i>} Se Hierarchical Columnar Superstructures for High-Performance Solar Cell Applications. Particle and Particle Systems Characterization, 2015, 32, 840-847.	1.2	34
51	Gallium doped <i>n</i> -type Zn _x Cd _{1-x} S nanoribbons: Synthesis and photoconductivity properties. Journal of Applied Physics, 2014, 115, 063108.	1.1	8
52	Porous CuCo ₂ O ₄ nanocubes wrapped by reduced graphene oxide as high-performance lithium-ion battery anodes. Nanoscale, 2014, 6, 6551-6556.	2.8	130
53	Surface Engineering of ZnO Nanostructures for Semiconductor‣ensitized Solar Cells. Advanced Materials, 2014, 26, 5337-5367.	11.1	149
54	n-Type KCu ₃ S ₂ microbelts: optical, electrical, and optoelectronic properties. RSC Advances, 2014, 4, 59221-59225.	1.7	6

Jun Xu

#	Article	IF	CITATIONS
55	Phase Conversion from Hexagonal CuS _{<i>y</i>} Se _{1â€"<i>y</i>} to Cubic Cu _{2â€"<i>x</i>} S _{<i>y</i>} Se _{1â€"<i>y</i>} : Composition Variation, Morphology Evolution, Optical Tuning, and Solar Cell Applications. ACS Applied Materials & amp; Interfaces, 2014, 6, 16352-16359.	4.0	46
56	Synthesis of Porous ZnS:Ag ₂ S Nanosheets by Ion Exchange for Photocatalytic H ₂ Generation. ACS Applied Materials & Interfaces, 2014, 6, 9078-9084.	4.0	128
57	Synthesis of Honeycombâ€like Mesoporous Pyrite FeS ₂ Microspheres as Efficient Counter Electrode in Quantum Dots Sensitized Solar Cells. Small, 2014, 10, 4754-4759.	5.2	83
58	One-pot synthesis of graphene/In2S3 nanoparticle composites for stable rechargeable lithium ion battery. CrystEngComm, 2013, 15, 6578.	1.3	28
59	Fluorinated Euâ€Doped SnO ₂ Nanostructures with Simultaneous Phase and Shape Control and Improved Photoluminescence. Particle and Particle Systems Characterization, 2013, 30, 332-337.	1.2	13
60	High performance nonvolatile memory devices based on Cu _{2â^'x} Se nanowires. Applied Physics Letters, 2013, 103, 193501.	1.5	13
61	Synthesis of In2O3–In2S3 core–shell nanorods with inverted type-I structure for photocatalytic H2 generation. Physical Chemistry Chemical Physics, 2013, 15, 12688.	1.3	61
62	CdS/CdSe Double-Sensitized ZnO Nanocable Arrays Synthesized by Chemical Solution Method and Their Photovoltaic Applications. Journal of Physical Chemistry C, 2012, 116, 2656-2661.	1.5	65
63	Large-scale synthesis of Cu2SnS3 and Cu1.8S hierarchical microspheres as efficient counter electrode materials for quantum dot sensitized solar cells. Nanoscale, 2012, 4, 6537.	2.8	101
64	Bimetallic PtPd nanoparticles on Nafion–graphene film as catalyst for ethanol electro-oxidation. Journal of Materials Chemistry, 2012, 22, 8057.	6.7	143
65	Polyvinylpyrrolidone-Assisted Ultrasonic Synthesis of SnO Nanosheets and Their Use as Conformal Templates for Tin Dioxide Nanostructures. Langmuir, 2012, 28, 10597-10601.	1.6	41
66	Cu ₂ ZnSnS ₄ Hierarchical Microspheres as an Effective Counter Electrode Material for Quantum Dot Sensitized Solar Cells. Journal of Physical Chemistry C, 2012, 116, 19718-19723.	1.5	193
67	Arrays of CdSe sensitized ZnO/ZnSe nanocables for efficient solar cells with high open-circuit voltage. Journal of Materials Chemistry, 2012, 22, 13374.	6.7	98
68	Microwave-assisted synthesis of Cu2ZnSnS4 nanocrystals as a novel anode material for lithium ion battery. Journal of Nanoparticle Research, 2012, 14, 1.	0.8	32
69	Tunable p-Type Conductivity and Transport Properties of AlN Nanowires <i>via</i> Mg Doping. ACS Nano, 2011, 5, 3591-3598.	7.3	47
70	Fabrication of highly ordered CuInSe2 films with hollow nanocones for anti-reflection. Applied Surface Science, 2011, 257, 10893-10897.	3.1	3
71	Arrays of ZnO/Zn _{<i>x</i>} Cd _{1–<i>x</i>} Se Nanocables: Band Gap Engineering and Photovoltaic Applications. Nano Letters, 2011, 11, 4138-4143.	4.5	185
72	Facile solution growth of vertically aligned ZnO nanorods sensitized with aqueous CdS and CdSe quantum dots for photovoltaic applications. Nanoscale Research Letters, 2011, 6, 340.	3.1	61

Јим Хи

#	Article	IF	CITATIONS
73	Synthesis of Homogeneously Alloyed Cu _{2â``<i>x</i>} (S _{<i>y</i>} Se _{1â^`<i>y</i>}) Nanowire Bundles with Tunable Compositions and Bandgaps. Advanced Functional Materials, 2010, 20, 4190-4195.	7.8	55
74	Simultaneous phase and size control of upconversion nanocrystals through lanthanide doping. Nature, 2010, 463, 1061-1065.	13.7	2,872
75	Low-Temperature Synthesis of CulnSe ₂ Nanotube Array on Conducting Glass Substrates for Solar Cell Application. ACS Nano, 2010, 4, 6064-6070.	7.3	86
76	Incorporation of Graphenes in Nanostructured TiO ₂ Films <i>via</i> Molecular Grafting for Dye-Sensitized Solar Cell Application. ACS Nano, 2010, 4, 3482-3488.	7.3	471
77	Large-Scale Synthesis and Phase Transformation of CuSe, CuInSe ₂ , and CuInSe ₂ /CuInS ₂ Core/Shell Nanowire Bundles. ACS Nano, 2010, 4, 1845-1850.	7.3	105
78	Largeâ€Scale Synthesis of Long Crystalline Cu _{2â€x} Se Nanowire Bundles by Waterâ€Evaporationâ€Induced Selfâ€Assembly and Their Application in Gas Sensing. Advanced Functional Materials, 2009, 19, 1759-1766.	7.8	137
79	Fabrication of Architectures with Dual Hollow Structures: Arrays of Cu ₂ 0 Nanotubes Organized by Hollow Nanospheres. Crystal Growth and Design, 2009, 9, 4524-4528.	1.4	34
80	Lithography inside Cu(OH)2 Nanorods:  A General Route to Controllable Synthesis of the Arrays of Copper Chalcogenide Nanotubes with Double Walls. Inorganic Chemistry, 2008, 47, 699-704.	1.9	48
81	Preparation, Conversion, and Comparison of the Photocatalytic and Electrochemical Properties of ZnS(en)0.5, ZnS, and ZnO. Crystal Growth and Design, 2007, 7, 280-285.	1.4	56
82	Mesoscale organization of Cu7S4 nanowires: Formation of novel sheath-like nanotube array. Chemical Physics Letters, 2007, 434, 256-259.	1.2	28
83	Controlled synthesis of CuO nanostructures by a simple solution route. Journal of Solid State Chemistry, 2007, 180, 1390-1396.	1.4	127
84	Optical properties of highly ordered AlN nanowire arrays grown on sapphire substrate. Applied Physics Letters, 2005, 86, 193101.	1.5	102